https://doi.org/10.1016/j.cep.2019.107561

Intensification and Performance Assessment for Synthesis of 2-Methoxy-2-Methyl-Heptane through the Combined Use of Different Pressure Thermally Coupled Reactive Distillation and Heat Integration Technique

Shirui Sun[a], Ao Yang[a], I-Lung Chien[b], Weifeng Shen[a,*], Shun'an Wei[a], Jingzheng Ren[c], and Xiangping Zhang[d]

[a]School of Chemistry and Chemical Engineering, Chongqing University, Chongqing 400044, China

[b]Department of Chemical Engineering, National Taiwan University, Taipei 10617, Taiwan

[c]Department of Industrial and Systems Engineering, The Hong Kong Polytechnic University, Hong Kong SAR, China

[d]Beijing Key Laboratory of Ionic Liquids Clean Process, CAS Key Laboratory of Green Process and Engineering, Institute of Process Engineering, Chinese Academy of Sciences, Beijing, 100190, PR China

Corresponding author: shenweifeng@cqu.edu.cn

Abstract: 2-methoxy-2-methyl-heptane (MMH) plays a key role in reformulated gasoline industry due to fewer environmental impacts than methyl *tert*-butyl ether. Thus, the design of MMH production process has received substantial attention. In this work, we propose a different pressure thermally coupled reactive distillation (DPTCRD) process for the synthesis of MMH aiming at reducing in energy requirements and improvement in environmental benefits. The key design variables are optimized to evaluate the economic feasibility of designed process. Furthermore, the heat integration strategy has been further explored by the application of heat exchanger network based on the observation of the temperature-enthalpy diagram to

fully utilize the redundant duty in DPTCRD system. The results demonstrate that the total annual cost of the heat integration-DPTCRD (HI-DPTCRD) is reduced by 29.17% than that of conventional reactive distillation process. In addition, CO_2 emission of the proposed HI-DPTCRD is decreased by 75.04% compared with that through the existing process.

Keywords: Energy-saving; Different pressure thermally coupled technique; Reactive distillation; Heat integration; 2-methoxy-2-methyl-heptane synthesis

Nomenclature

MMH	2-methoxy-2-methyl-heptane
MTBE	methyl *tert*-butyl ether
MH	2-methyl-1-heptene
MeOH	methanol
DME	dimethyl ether
MHOH	2-methyl-2-heptanol
TAC	total annual cost
RD	reactive distillation
HI-RD	heat integration-RD
DPTCRD	different pressure thermally coupled reactive distillation
HPC	high-pressure column
LPC	low-pressure column
VLE	vapor-liquid equilibrium
HEN	heat exchanger network

HI-DPTCRD	heat integration-DPTCRD
HCC	hot composition curve
CCC	cold composition curve

1. Introduction

As a new candidate of oxygenated fuel additive, 2-methoxy-2-methyl-heptane (MMH) has significant advantages in boosting octane number in gasoline than methyl *tert*-butyl ether (MTBE) [1]. Moreover, MMH can effectively avoid the groundwater contamination problems caused by MTBE due to the higher molecular weight that exhibits significantly decreased solubility [2]. Therefore, to gain financial and environmental benefits, the synthesis of MMH has received considerable attention from chemical and petroleum industries [1-3].

Generally, MMH is produced by 2-methyl-1-heptene (denoted as MH) and methanol (called as MeOH) reacting in an etherification reaction system [4]. It is also worth noting that the reaction of MeOH and MH to produce two by-products dimethyl ether (represented as DME) and 2-methyl-2-heptanol (i.e. MHOH) is undesirable. Thus, several effective designs such as excess of MH have been investigated to obtain the desired product MMH with higher yields. However, large capital and energy investments are demanded in those designs. To overcome the above mentioned problem, Griffin et al. [4] explored the relationship of equilibrium constant and optimum design parameters in the production of MMH. Following that, the optimum parameters (i.e. reactor sizes and the ratio of recycle and feed flowrate) have been investigated to save capital and operating costs [2]. Besides, the integration of

reaction and separation process into one single operation vessel is called as reactive distillation (RD) attracted considerable attentions in the reduction of capital costs and energy consumption. In addition, RD has dominating advantages in the reversible reaction due to the increasing of reaction equilibrium by quickly removing products [5, 6]. Thus, RD process has been investigated by many studies [7-10]. For instance, Moraru et al. [11] proposed an energy-efficient RD for the synthesis of 2-Ethylhexyl acrylate and they demonstrated that the energy investments of the RD process are decreased by 22.22% compared with the reaction-separation-recycle process. The feasibility of RD for MMH production has been proved and an intensified RD configuration with different heat integration sequences has be proposed [3], which can save 36.7% in energy consumption than that of convention process.

To further reduce energy consumptions, several energy-saving approaches such as reactive dividing-wall column [12-14], vapor recompression heat pump RD [15-17], and different pressure thermally coupled reactive distillation (DPTCRD) [13, 18, 19] have been investigated. Generally, the RD column is divided into a high-pressure column (HPC) and a low-pressure column (LPC) in DPTCRD process to satisfy the demand of heat transfer temperature difference resulting in the heat-integration of top vapor stream from HPC and reboiler of LPC. The synthesis of *tert*-amyl methyl ether using DPTCRD has been investigated and it saved 6.56% of TAC compared with traditional RD process [20]. Li et al. investigated the application of attractive DPTCRD technique in the hydrolysis of methyl acetate leading to TAC savings of 7.49% [19].

As is well known, heat integration technique as another effective tool to enhance energy efficiency and reduce energy investments in distillation system has recently attracted considerable attentions [21-27]. For example, Gu et al. explored the application of heat integration in an energy-efficient lower pressure extractive distillation for separating tetrahydrofuran-methanol-water mixture [28]. The combination of heat integration and vapor recompression design for pressure swing distillation has been investigated to improve energy efficiency [29]. Novita et al. [23] proposes an energy-saving process for the synthesis of ethyl levulinate using the thermally coupled RD with heat integration resulting in TAC savings of 10.5% compared with conventional RD process.

The contribution of this study is proposing a novel MMH production process through reactive distillation combining DPTC and heat integration technologies, which makes full use of latent and sensible heats in this system and achieves better economic and environmental performance. Moreover, a systematic procedure including design, optimization, heat-integration analysis and evaluation for the novel MMH production process is presented. Firstly, the DPTCRD process for MMH synthesis is design to save energy consumptions and capital costs. Then, sequential iterative optimization is applied to obtain optimal key design variables. Following that, the analysis of the temperature-enthalpy diagram and heat exchange network aiming to improve energy efficiency is utilized to design the heat-integration scheme for DPTCRD process to further save energy consumption. Finally, the TAC and CO_2 emission are introduced to evaluate the proposed configurations from economic and

environmental aspects.

2. The existing MMH production process

Hussain et al. [3, 30] proposed the RD configurations for the synthesis of MMH to achieve lower energy costs and TAC, as illustrated in Fig. 1. The RD column including reactive and stripping section has 35 total stages operated at 1.77 atm. Notice that reactive section runs from stage 2 to stage 12. The low-boiling reactant MeOH stream is introduced at the bottom of the reaction section (i.e., stage 13), while the MH stream combined with a recycle stream is fed at stage 1. The distillate from the RD column is fed at stage 5 of C2 column. Column C2 with a 12 stages aims to deliver high-purity DME as the distillate. Column C3 with 15 stages receives a feed stream at the stage 8 from the bottom of the RD column. The distillate product of Column C3 is MMH with 99.9 mol% while the bottom is undesired MHOH with 99.9 mol%. To further save energy consumption, Hussain et al. explored the heat-integration scheme of RD process [3]. Fig. 2 describes the best heat-integration RD (HI-RD) process for MMH production.

3. Methodology

We propose a systematic procedure for optimal design and evaluation of the MMH synthesis process by combining DPTCRD and heat integration technologies, as described in Fig. 3. First, the existing MMH production process (i.e. RD process) is simulated as a reference to verify the economic feasibility of alternative process. Next, alternative configuration combining the energy-saving technique with existing RD process is proposed to save energy consumptions. Then, the process simulation and

optimization are performed to obtain optimal key operational design parameters. Following that, heat integration for the proposed alternative configuration has been investigated to further save energy costs. Finally, the economic and CO_2 emission evaluation are applied for the comparison of the existing MMH production process and proposed alternative configurations from both financial and environmental views.

3.1 Reaction kinetics and thermodynamics

In the MMH synthesis reaction system, MMH is produced by the reversible etherification reaction of MH with MeOH, which is expressed in Eq. 1. However, an irreversible reaction between MeOH and MH represented by Eq. 2 occurs in this system resulting in the production of DME and MHOH.

$$\mathrm{MeOH + MH \leftrightarrow MMH} \tag{1}$$

$$\mathrm{MeOH + MH \rightarrow DME + MHOH} \tag{2}$$

The kinetics for MMH etherification reaction has been investigated by Luyben [2] and Griffin et.al [4]. The reaction mechanism over an acid resin catalyst Amberlyst 35Wet is described by a pseudo-homogenous model based on the catalyst weight and mole fraction (x) of the components involved [31]. The corresponding rate equations can be expressed as Eqs. 3 and 4,

$$r_1 = k_{1f} \cdot x_{\mathrm{MeOH}} \cdot x_{\mathrm{MH}} - k_{1r} \cdot x_{\mathrm{MMH}} \tag{3}$$

$$r_2 = k_2 \cdot (x_{\mathrm{MeOH}})^2 \tag{4}$$

where r_1 and r_2 are the reaction rates of two reactions involving in the etherification of MeOH with MH. k_{1f} and k_{1r} are the forward and reverse reaction rate constant of the reaction for synthesizing MMH, respectively. k_2 stands for the reaction rate constant

of the side reaction to produce DME and MHOH. Table 1 presents detailed kinetic parameters in Eqs. (3) and (4). Notice the activation energy of the forward reaction is larger than that of the reverse reaction. Therefore, high reactive temperature is beneficial for increasing of conversion. However, the reactive temperature must be lower than permissible catalyst deactivation temperature (423 K) [3]. In this work, the catalyst loading is 600 kg/stage in reactive section.

Herein, the simulation of MMH production process is conducted via a rigorous model provided by Aspen Plus. Of note is that components MMH and MHOH are not available in the Aspen databank. As such, both MMH and MHOH are generated via the molecular structures (shown in Fig. 4). In the MMH synthesis system, the UNIQUAC activity coefficient model has been utilized to describe the vapor-liquid equilibrium (VLE) relationship following the suggestion of Luyben [2]. However, only binary interaction parameters between MeOH and DME are available in the built-in UNIQUAC thermodynamic model. Thus, other separations revolved in this study are assumed as ideal VLE behavior according to the study of Hussain et al. [3].

3.2 Proposed novel DPTCRD configuration

Distillation technologies have been widely used for separating liquid mixtures in petroleum and chemical industries, whose major obstacle is the huge energy requirements [2]. RD has been investigated to achieve high energy-efficiency via the comprehensive utilization of the reaction heat. Aiming to further reduce the energy requirements, several energy-saving methods (e.g. DPTCRD, dividing-wall distillation and heat-integration techniques) have been applied to RD process [10].

Thus, we propose a novel DPTCRD process for the synthesis of MMH to save energy costs.

The application of DPTCRD in the synthesis process of MMH to reduce capital costs and energy investments is presented in Fig. 5. The RD column is divided into an HPC worked as reactive section and an LPC served as stripping section. The bottom liquid stream of the HPC flows into the top of the LPC and the top vapor stream of the LPC is compressed and then driven to the bottom of the HPC. The latent duty of top vapor stream in HPC is used as the heat source for the reboiler of the LPC. The distillate in the HPC is fed to C2 column to deliver the high-purity DME as the by-product, while the unreacted MH containing a little bit of MeOH is recycled to HPC. The bottom stream in the LPC is fed to C3 column to obtain the product MMH with a purity of 99.9 mol%. To make a fair comparison, the yield of MMH in proposed DPTCRD process is set to 99% to keep same with that of existing MMH-RD process.

3.3 Process simulation and optimization for DPTCRD

The simulation of the proposed process for MMH production based on the existing RD process has been conducted [3], and the results are used to provide a starting point for the simulation of proposed alternative process. Table 2 illustrates the design parameters of RD process. The DPTCRD process for MMH production consisted of four columns (i.e. HPC, LPC, C2 and C3) and a single compressor, which designed as the following steps:

(1) Divide the RDC into HPC and LPC. The operating pressure of HPC is same

with RDC while the operating pressure of LPC is decreased to meet heat transfer requirements.

(2) Drag a vapor stream that leaves the LPC from stage 1 and connect it to the compressor whilst output stream is connected to the bottom of the HPC.

(3) Set an outlet pressure compressor equaling to the pressure of the bottom in HPC.

(4) Set one design specification using Design Spec/Vary function until satisfying the specified yield through varying the flowrate of vapor stream driven to HPC.

(5) Set four design specification for C2 and C3 column using Design Spec/Vary function until satisfying the specified mole purities of DME, MH recycle, MHOH and MMH through varying the distillate rate and reflux ratio of C2 and C3 column.

In the preliminary design of DPTCRD process, the design variables (i.e. the total number of stages, feed locations and operating pressure etc.) are kept same with RD process and will been further optimized. More detailed descriptions on the design of equipment size are presented in section 3.5 Economic and CO_2 emissions evaluation.

Sequential iterative optimization is utilized in this study to determine optimal design variables under the specified product purities. In this system, the design variables include the total stages of LPC (NLPC), total stages of C2 (NC2), total stages of C3 (NC3), the feed locations of C2 (NFC2) and C3 (NFC3). According to the study of Wang et al. [32], this optimization procedure consists of the inner iterative loop (NFC3 and NFC2) and the outer iterative loop (NLPC, NC2 and NC3). The procedure of sequential iterative optimization for the DPTCRD system is

presented in Fig. 6. During the optimization, the mole purities of MMH, MHOH, DME and MH recycle are defined in the 'Design Spec' function to meet their product specifications by manipulating the reflux ratio and distillate rate of C2 and C3, respectively. TAC is defined as the objective function via 'Calculator Tools/Fortran' in Aspen Plus [33, 34]. The lower and upper bonds of design variables are adjusted if the TAC is not obtaining the minimum value in optimizing procedure. After all design variables was well optimized by this procedure, the minimum TAC and corresponding design variable would be obtained [35].

3.4 The heat integration of optimal DPTCRD

Heat integration between process streams can bring both economic benefits (i.e., the lower energy consumption) and environmental benefits (i.e., a reduction in CO_2 emissions) [36]. Firstly, a temperature-enthalpy diagram as an efficient tool in the analysis of the energy consumption and utility requirements is utilized to illustrate the feasibility of heat integration. Then, to comprehensively utilize the heat duty of hot streams in the process, heat exchanger network (HEN) using pinch analysis has been explored to save investments of energy [37]. Finally, the heat integration-DPTCRD (HI-DPTCRD) process with the optimal HEN is simulated to verify the feasibility of the HI-DPTCRD.

3.5 Economic and CO_2 emissions evaluation

TAC, as most frequently criteria in the financial evaluation for chemical process, is introduced to assess the economic performance of different designs and detailed economic analysis in terms of TAC is presented in this section. TAC is defined by Eq.

5 [9, 38].

$$\mathrm{TAC} = \frac{\mathrm{CC}}{\text{payback period}} + \mathrm{EC} \tag{5}$$

where *CC* denotes capital costs summing up the cost of column shell, trays, condensers, reboilers, heat exchangers and compressor. The detailed calculation of equipment sizing and capital costs estimating formulas are shown in Table 3 [10, 38-42]. Aspen tray sizing is utilized to estimate the column diameters of LPC, C2 and C3 with the maximum flooding of 80% and the number of theory trays is adopted for calculating the column height with the tray spacing in the columns of 0.6096 m. Each reactive stage in the RDC involves liquid holdup of 0.75 m^3 that gives a weir height of 0.152 m for the RDC with a diameter of 3.74 m. EC denotes annualized energy cost including the costs of steam, coolant, catalyst and electricity. The corresponding utility prices are illustrated in Table 3 [24, 38]. Herein, the payback period is set as 3 years to make a fair comparison with the work of Hussain et al. [3], and the total annual operating time is assumed to be 7920 h.

To comprehensively evaluate the proposed DPTCRD process, the environmental impact and sustainability of the alternative process should be investigated [43]. Therefore, CO_2 emissions evaluation is introduced in the proposed MMH synthesis process. Generally, the steam used for reboiler in distillation system can be generated by the traditional energy resources (i.e. coal, heavy fuel oil and nature gas). However, it is difficult to evaluate CO_2 emissions for the process involving in vapor recompression system because both steam turbine and electricity driving can provide the power of compressor. Besides, both traditional and new energy resources can be

utilized to generate electricity. Herein, to make a fair comparison, two assumptions are made: (1) the steam used in reboiler for MMH production system is generated by heavy fuel oil, and (2) CO_2 emission for the 1000 kW electricity power of a compressor is set as 184 kg/h [17]. Following the suggestions of Gadalla et al. [44, 45], the CO_2 emissions in MMH process have been calculated via Eq. 6.

$$(CO_2)_{emissions} = (\frac{Q_{fuel}}{NHV}) \times (\frac{C\%}{100})\alpha \quad (6)$$

where α represents the molar masses ratio of CO_2 and C, which is set as 3.67. The NHV denotes an abbreviation of net heating value and C% is carbon content. In this study, NHV is 39771 kJ/kg because heavy fuel oil has been used to generate steam, and the carbon content is 86.5 kg/kg. Q_{fuel} denotes the heat duty of fuel required in this system and can be calculated by Eq. 7.

$$Q_{fuel} = \frac{Q_{seq}}{\lambda_{seq}} \times (h_{seq} - 419) \times (\frac{T_F - T_0}{T_F - T_S}) \quad (7)$$

where λ_{seq} (kJ/kg) is latent heat of the steam, h_{seq} denotes enthalpy of the steam and Q_{seq} (kJ) is the energy requirements in this process. T_F, T_S and T_0 represent the flame temperature (2073.15 K), the stack temperature (433.15 K) and the standard temperature (298.15 K), respectively.

4 Computational results and discussion

4.1 Simulation and optimization of the proposed DPTCRD process

The ratio of MeOH and MH flow rate is essential for the DPTCRD process due to its significantly influence on MMH yield and the determination of pressure in DPTCRD. The fresh MH and MeOH flowrates are kept same with existing RD

process. Thus, the MH recycle is determined firstly. TAC is set as objective function to find optimal MH recycle rate. Of note is that there are two design specifications to meet MMH yield and the demands of temperature difference for heat transfer. Fig.7 shows the effect of MH recycle flow rate on TAC. It is obvious that the optimal MH recycle flow rate is 40.98 kmol/h.

Pressures in the HPC and LPC are essential for the DPTCRD process due to the significantly influence in the product purities and energy requirements [46]. The temperature of bottom stream in LPC is descended with the reduction of pressure of LPC, which provides a potential for heat integration between the top vapor stream in HPC and bottom liquid stream in LPC. To achieve the requirement of heat transfer, the temperature difference is set to be greater than 8.0 K [10]. Fig. 8 illustrates the effects of P_{LPC} on compressor duty, compress ratio, heat transfer temperature difference, and condenser duty of the HPC and reboiler duty of the LPC. Fig. 8a presents that the pressure ratio is increasing with the decrease in the pressure of LPC. As shown in Fig. 8b, the compressor duty is increasing with the increase in the pressure ratio indicating more equipment investment is demanded. On the other hand, The bottom temperature of the LPC varies from 387.4 to 395.0 K with the P_{LPC} increases from 0.34 to 0.43 atm, while the top temperature of the HPC maintains at around 401.9 K, leading to the decrease of the heat transfer temperature difference. Thus, P_{LPC} should be decreased as far as possible on the premise of achieving minimum heat transfer temperature difference, which is selected as 0.41 atm in this work. Fig. 8 (d) shows that the condenser duty of the HPC is always more than the

reboiler duty of the LPC, which means that the reboiler duty for the LPC can be completely provided by the top vapor stream of the HPC. To make a fair comparison, the feed conditions and product specifications in DPTCRD process are consistent with those in the existing RD process. The flowsheet of the DPTCRD configuration is depicted in Fig. 9.

In this process, the LPC is operated at 0.41 atm and the reboiler duty of LPC is 0.85 MW. The HPC is operated at 1.77 atm with the condenser duty of HPC is 2.69 MW. A compressor provided 0.32 MW with compressor ratio of 4.32. Of note is that the temperature difference between the condenser in HPC and the reboiler in LPC is 8.5 K, meeting the demand of a normal heat transfer [47]. Thus, the reboiler duty of LPC is provided by the vapor of HPC and the redundant duty of HPC is provided by cooling water. The mixture D1 is then sent into the column C2 at pressure 10 atm, high purity of DME is obtained at the top stream and MH with 99.9 mol% at bottom stream is recycled to the HPC. Stream B1 is fed to the column C3 at pressure 0.1 atm to obtain MMH with 99.9 mol% at overhead stream and high purity of MHOH is obtained at the bottom stream.

Then, the optimal design parameters are obtained through sequential iterative optimization procedure. The effects of the total stages of LPC (N_{LPC}), the total stages of C2 (N_{C2}), the total stages of C3 (N_{C3}), and the feed locations of C2 (N_{FC2}) and C3 (N_{FC3}) on the TAC are illustrated in Fig. 10. It can be observed that the rapidly reduction on TAC when N_{LPC} increases from 20 to 23 and the TAC increases when N_{LPC} increases from 23 to 25. Therefore, the optimal total stage of LPC is selected as

23. Similar observations can be used for the other four parameters from Fig. 9. Thus, the optimal N_{C2}, N_{C3}, N_{FC2} and N_{FC3} are 11, 15, 5 and 6, respectively. At the same time, optimal mole reflux ratios of C2 and C3 are 1.15 and 0.105 via 'Design Spec' function in Aspen Plus.

The liquid composition profile and temperature profiles of the proposed DPTCRD process demonstrated in Figs. 11 and 12. From Fig. 11 (a), the bottom product at stage 21 of LPC contains MMH (desired) with 98.9 mol% and a little bit of the MHOH product (undesired). Unreacted MeOH and excess MH together with by-product DME is obtained at the top of HPC, as shown in Fig. 11 (c). The unreacted MH will be recycled to the HPC after purifiing by C3 column. From Fig. 11 (b), the temperature in the bottom of the reaction section (i.e., stage 13) is lower than the permissible catalyst deactivation temperature (423 K). From Fig. 12 (a) and (c), the distillate of C2 column is DME with the purity of 99.9 mol%, and the distillate of C3 column is MMH with the purity of 99.9 mol% while the bottom of C3 column is MHOH with 99.9 mol%.

4.2 Heat integration of the optimized DPTCRD process

Fig. 13 shows the temperature-enthalpy diagram of the DPTCRD process. The hot composition curve (HCC) marked as the red solid lines represents the available heat in this DPTCRD system and the cold composition curve (CCC) marked as blue solid lines denotes the heat demands of the process. Q_{FH} indicates the hot utility demands (i.e., low-pressure steam) and Q_{CW} denotes the cold utility requirements (i.e., cooling water) of the DPTCRD process and they are 0.39 MW and 2.03 MW,

respectively. The maximum possible heat recovery in the DPTCRD process (described by the shadowed area in Fig. 13) is 1.29 MW.

In an attempt to reduce the requirements of energy in DPTCRD process and improve energy integration between process streams, the design of HEN has been developed by application of graphical pinch-analysis method [48]. The HEN design of DPTCRD process is implemented in Aspen Energy Analyzer. According to the temperature-enthalpy diagram in MMH production system, the top stream of HPC can be utilized to heat the bottom stream of LPC and C3 and the it can use either a series or a parallel arrangement. However, from a dynamic control perspective, the series configuration suffers from problems of interaction between the units [49]. Thus, we choose parallel configuration in this paper to avoid fluid mechanics and heat-transfer problems because of the complexities of two-phase flow and heat transfer. The final HEN of the DPTCRD process is presented in Fig. 14. The system is composed of six heat exchanger units. E1 and E6 are self-heat exchangers while E2, E3 and E5 are coolers utilizing cooling water. E4 is heater using high-pressure steam. The heating and cooling requirements of the optimal HEN are 0.39 MW and 2.03 MW, respectively. The final flowsheet of DPTCRD with the optimized HEN is demonstrated in Fig. 15. The HI-DPTCRD process can respectively save 26.19% of Q_{FH} and 17.85% of Q_{CW} than those of DPTCRD process.

4.3 Economic and CO_2 emissions evaluations

The detailed economic evaluations including capital and energy costs of the four configurations and individual units are shown in Fig. 16 and Table 4, respectively. It

can be observed that two proposed DPTCRD and HI-DPTCRD configurations have dominating advantages in economic benefits and energy consumption compared with those of the RD configuration. The RD column is divided into an HPC and an LPC, and the duty of reboiler in LPC reduces with the decrease in operation pressure leading to lower energy consumption. Moreover, energy cost can be further decreased by the heat-integration of DPTCRD process in which the redundant duty of the vapor stream in HPC is utilized as heat source for the bottom streams of LPC and C2. Compared with the RD process, energy costs of proposed DPTCRD and HI-DPTCRD process are decreased by 33.53% and 45.76%, respectively. In fact, TAC includes both energy costs and capital costs. Hereby, compared with the RD process, the TAC of proposed DPTCRD and HI-DPTCRD process are reduced by 23.80% and 29.17%, respectively. In addition, the TAC of HI-DPTCRD process is saving by 20.01% compared with HI-RD process. The computational results illustrate that the HI-DPTCRD is the most promising configuration among the four MMH production processes due to the higher thermodynamic efficiency in reducing the energy requirements of the rebolier.

The CO_2 emissions of proposed two alternative configurations and the existing RD and HI-RD process have been illustrated in Table 5. The CO_2 emissions of HI-RD process decreases by 24.34%. Compared with existing RD process, the CO_2 emissions of proposed DPTCRD and HI-DPTCRD configurations for MMH synthesis process are respectively reduced by 55.57% and 75.04%, respectively. This significant reduction mainly attributes to the reduction in total reboiler duties of the alternative

designs.

5 Conclusions

A novel process combining different pressure thermally coupled reactive distillation (DPTCRD) and heat-integration technology for the synthesis of 2-methoxy-2-methyl-heptane (MMH) is proposed in this work. Firstly, the DPTCRD process is designed and optimized to save energy and capital costs. To further save energy consumptions, the temperature-enthalpy diagram is used to analyze the energy-saving potential of the alternative process and the heat exchange network is then utilized to design the optimal heat integration of the DPTCRD process.

Reactive distillation (RD), DPTCRD and heat integration-DPTCRD (HI-DPTCRD) processes are comprehensively evaluated from the views of financial and environmental performances. The results demonstrate that HI-DPTCRD process is the most promising configuration among the four approaches for the MMH production. Due to the decrease both in capital and energy costs, the TAC of HI-DPTCRD process can be reduced by 29.17% and 7.02% compared with those of the RD and DPTCRD processes, respectively. In addition, it is found that the CO_2 emissions of the proposed HI-DPTCRD configuration can reduce 75.04% compared with that of the RD process owing to the reduction in energy consumptions.

It is worth mentioning that the proposed process may be not suitable for the RD process that have the large temperature difference between top vapor stream and bottom liquid stream because a huge capital costs is needed in this process. However, the proposed method for the HI-DPTCRD configuration could be widely extended to

other similar processes such as reactive dividing wall column to achieve reduction in TAC and sustainable development.

Acknowledgment

We acknowledge the financial support provided by the National Natural Science Foundation of China (Nos. 21606026, 21878028); the Chongqing Research Program of Basic Research and Frontier Technology (No. CSTC2016JCYJA0474); the Chongqing Innovation Support Program for Returned Overseas Chinese Scholars (No. CX2018048); the Beijing hundreds of leading talents training project of science and technology (No. Z171100001117154)

References

[1] A. Hussain, M. Lee, Optimal design of an intensified column with side-reactor configuration for the methoxy-methylheptane process, Chem. Eng. Res. Des. 136 (2018) 11-24.

[2] W.L. Luyben, Design and Control of the Methoxy-Methyl-Heptane Process, Ind. Eng. Chem. Res. 49 (2010) 6164-6175.

[3] A. Hussain, L.Q. Minh, M.A. Qyyum, M. Lee, Design of an Intensified Reactive Distillation Configuration for 2-Methoxy-2-methylheptane, Ind. Eng. Chem. Res. 57 (2017) 316-328.

[4] D.W. Griffin, D.A. Mellichamp, M.F. Doherty, Effect of Competing Reversible Reactions on Optimal Operating Policies for Plants with Recycle, Ind. Eng. Chem. Res. 48 (2009) 8037-8047.

[5] S. Kai, A. Kienle, Reactive Distillation: Status and Future Directions, Rims Kokyuroku, 1330 (2003) 134-148.

[6] J.G. Segovia-Hernández, S. Hernández, A.B. Petriciolet, Reactive distillation: A review of optimal design using deterministic and stochastic techniques, Chem. Eng. Process. Process Intensif. 97 (2015) 134-143.

[7] V. Feyzi, M. Beheshti, Exergy analysis and optimization of reactive distillation column in acetic acid production process, Chem. Eng. Process. Process Intensif. 120 (2017) 161-172.

[8] C. Gutiérrez-Antonio, M.L. Soria Ornelas, F.I. Gómez-Castro, S. Hernández, Intensification of the hydrotreating process to produce renewable aviation fuel through reactive distillation, Chem. Eng. Process. Process Intensif. 124 (2018) 122-130.

[9] A. Yang, L. Lv, W. Shen, L. Dong, J. Li, X. Xiao, Optimal Design and Effective Control of the tert-Amyl Methyl Ether Production Process Using an Integrated Reactive Dividing Wall and Pressure Swing Columns, Ind. Eng. Chem. Res. 56 (2017) 14565-14581.

[10] A. Yang, S. Sun, A. Eslamimanesh, S.a. Wei, W. Shen, Energy-saving investigation for diethyl carbonate synthesis through the reactive dividing wall column combining the vapor recompression heat pump or different pressure thermally coupled technique, Energy, 172 (2019) 320-332.

[11] M.D. Moraru, C.S. Bildea, Process for 2-Ethylhexyl Acrylate Production Using Reactive Distillation: Design, Control, and Economic Evaluation, Ind. Eng. Chem. Res. 57 (2018) 2609-2627.

[12] J.A. Weinfeld, S.A. Owens, R.B. Eldridge, Reactive dividing wall columns: A comprehensive review, Chem. Eng. Process. Process Intensif. 123 (2018) 20-33.

[13] Q. Zhang, T. Guo, C. Yu, Y. Li, Design and control of different pressure thermally coupled reactive distillation for amyl acetate synthesis, Chem. Eng. Process. Process Intensif. 121 (2017) 170-179.

[14] J. Xie, F. Peng, C. Li, T. Jiang, S. Ma, Coproduction of Ethyl Acetate and n -Butyl Acetate by Using a Reactive Dividing-Wall Column, Chem. Eng. Technol. 41 (2018) 1808-1817.

[15] S. Sharma, D.S. Patle, A.P. Gadhamsetti, S. Pandit, D. Manca, N. G S, Intensification and performance assessment of the formic acid production process through a dividing wall reactive distillation column with vapor recompression, Chem. Eng. Process. Process Intensif. 123 (2018) 204-213.

[16] S. Feng, Q. Ye, H. Xia, R. Li, X. Suo, Integrating a vapor recompression heat pump into a lower partitioned reactive dividing-wall column for better energy-saving performance, Chem. Eng. Res. Des. 125 (2017) 204-213.

[17] M.A. Waheed, A.O. Oni, S.B. Adejuyigbe, B.A. Adewumi, D.A. Fadare, Performance enhancement of vapor recompression heat pump, Appl. Energy 114 (2014) 69-79.

[18] G. Contreras-Zarazúa, J.A. Vázquez-Castillo, C. Ramírez-Márquez, G.A. Pontis, J.G. Segovia-Hernández, J.R. Alcántara-Ávila, Comparison of intensified reactive distillation configurations for the synthesis of diphenyl carbonate, Energy, 135 (2017) 637-649.

[19] L. Li, L. Sun, J. Wang, J. Zhai, Y. Liu, W. Zhong, Y. Tian, Design and Control of Different Pressure Thermally Coupled Reactive Distillation for Methyl Acetate Hydrolysis, Ind. Eng. Chem. Res. 54 (2015) 12342-12353.

[20] X. Gao, F. Wang, H. Li, X. Li, Heat-integrated reactive distillation process for TAME synthesis, Sep. Sci. Technol. 132 (2014) 468-478.

[21] T. Chen, B. Zhang, Q. Chen, Heat integration of fractionating systems in para-xylene plants based on column optimization, Energy, 72 (2014) 311-321.

[22] J. Gu, X. You, C. Tao, J. Li, W. Shen, J. Li, Improved design and optimization for separating tetrahydrofuran–water azeotrope through extractive distillation with and without heat integration by varying pressure, Chem. Eng. Res. Des. 133 (2018) 303-313.

[23] F.J. Novita, H.-Y. Lee, M. Lee, Energy-Efficient Design of an Ethyl Levulinate Reactive Distillation Process via a Thermally Coupled Distillation with External Heat Integration Arrangement, Ind. Eng. Chem. Res. 56 (2017) 7037-7048.

[24] A. Yang, R. Wei, S. Sun, S.a. Wei, W. Shen, I.L. Chien, Energy-Saving Optimal Design and Effective Control of Heat Integration-Extractive Dividing Wall Column for Separating Heterogeneous Mixture Methanol/Toluene/Water with Multiazeotropes, Ind. Eng. Chem. Res. 57 (2018) 8036-8056.

[25] M. Yang, X. Feng, G. Liu, Heat integration of heat pump assisted distillation into the overall process, Appl. Energy 162 (2016) 1-10.

[26] Z. Zhu, L. Wang, Y. Ma, W. Wang, Y. Wang, Separating an azeotropic mixture of toluene and ethanol via heat integration pressure swing distillation, Comput. Chem. Eng. 76 (2015) 137-149.

[27] Y. Jiao, S.-J. Wang, K. Huang, H. Chen, W. Liu, Design and Analysis of Internally Heat-Integrated Reactive Distillation Processes, Ind. Eng. Chem. Res. 51 (2012) 4002-4016.

[28] J. Gu, X. You, C. Tao, J. Li, V. Gerbaud, Energy-Saving Reduced-Pressure Extractive Distillation with Heat Integration for Separating the Biazeotropic Ternary Mixture Tetrahydrofuran–Methanol–Water, Ind. Eng. Chem. Res. 57(2018) 13498-13510.

[29] B. Kiran, A.K. Jana, Assessing the performance improvement of an intensified heat integration scheme: Reactive pressure-swing distillation, Appl. Therm. Eng. 76 (2015) 509-520.

[30] A. Hussain, M.A. Qyyum, H. Jimin, M. Lee, A novel design of reactive distillation configuration for 2-methoxy-2-methylheptane process, in: E3S Web of Conferences, EDP Sciences, 2017, pp. 00067.

[31] R.S. Karinen, A.O.I. Krause, Reactivity of some C8-alkenes in etherification with methanol, Applied Catalysis A: General, 188 (1999) 247-256.

[32] Y. Wang, G. Bu, X. Geng, Z. Zhu, P. Cui, Z. Liao, Design optimization and operating pressure effects in the separation of acetonitrile/methanol/water mixture by ternary extractive distillation, J. Clean. Prod. 218 (2019) 212-224.

[33] L. Zheng, W. Cai, X. Zhang, Y. Wang, Design and control of reactive dividing-wall column for the synthesis of diethyl carbonate, Chem. Eng. Process. Process Intensif. 111 (2017) 127-140.

[34] A. Yang, W. Shen, S.a. Wei, L. Dong, J. Li, V. Gerbaud, Design and control of pressure-swing distillation for separating ternary systems with three binary minimum azeotropes, AIChE J. 65 (2019) 1281-1293.

[35] T. Shi, A. Yang, S. Jin, W. Shen, S.a. Wei, J. Ren, Comparative optimal design and control of two alternative approaches for separating heterogeneous mixtures isopropyl alcohol-isopropyl acetate-water with four azeotropes, Sep. Purif. Technol.

225 (2019) 1-17.

[36] O. Aboelazayem, M. Gadalla, B. Saha, Design and simulation of an integrated process for biodiesel production from waste cooking oil using supercritical methanolysis, Energy, 161 (2018) 299-307.

[37] L.V. Pavão, C.B.B. Costa, M.A.S.S. Ravagnani, Heat Exchanger Network Synthesis without stream splits using parallelized and simplified simulated Annealing and Particle Swarm Optimization, Chem. Eng. Sci. 158 (2017) 96-107.

[38] J.M. Douglas, Conceptual design of chemical processes, McGraw-Hill New York, 1988.

[39] Ž. Olujić, L. Sun, A. de Rijke, P.J. Jansens, Conceptual design of an internally heat integrated propylene-propane splitter, Energy, 31 (2006) 3083-3096.

[40] Z. Feng, W. Shen, G.P. Rangaiah, L. Lv, L. Dong, Process Development, Assessment, and Control of Reactive Dividing-Wall Column with Vapor Recompression for Producing n-Propyl Acetate, Ind. Eng. Chem. Res. 58 (2018) 276-295.

[41] X. You, J. Gu, V. Gerbaud, C. Peng, H. Liu, Optimization of pre-concentration, entrainer recycle and pressure selection for the extractive distillation of acetonitrile-water with ethylene glycol, Chem. Eng. Sci. 177 (2018) 354-368.

[42] Y. Hu, Y. Su, S. Jin, I.L. Chien, W. Shen, Systematic approach for screening organic and ionic liquid solvents in homogeneous extractive distillation exemplified by the tert-butanol dehydration, Sep. Purif. Technol. 211 (2019) 723-737.

[43] A. Yang, H. Zou, I.L. Chien, D. Wang, S.a. Wei, J. Ren, W. Shen, Optimal Design and Effective Control of Triple-Column Extractive Distillation for Separating Ethyl Acetate/Ethanol/Water with Multiazeotrope, Ind. Eng. Chem. Res. 58 (2019) 7265-7283.

[44] M. Gadalla, Z. Olujic, M. Jobson, R. Smith, Estimation and reduction of CO2 emissions from crude oil distillation units, Energy, 31 (2006) 2398-2408.

[45] M. Gadalla, Z. Olujic, A. Derijke, P. Jansens, Reducing CO2 emissions of internally heat-integrated distillation columns for separation of close boiling mixtures, Energy, 31 (2006) 2409-2417.

[46] L. Liu, L. Zhu, L. Sun, M. Zhu, G. Liu, Simulation and optimization of different pressure thermally coupled distillation for separating a close-boiling mixture of n-butanol and iso-butanol, Applied Petrochemical Research, 7 (2017) 143-150.

[47] W.L. Luyben, Comparison of flowsheets for THF/water separation using pressure-swing distillation, Comput. Chem. Eng. 115 (2018) 407-411.

[48] S.-G. Yoon, J. Lee, S. Park, Heat integration analysis for an industrial ethylbenzene plant using pinch analysis, Appl. Therm. Eng. 27 (2007) 886-893.

[49] W.L. Luyben, Series versus parallel reboilers in distillation columns, Chem. Eng. Res. Des. 133 (2018) 294-302.

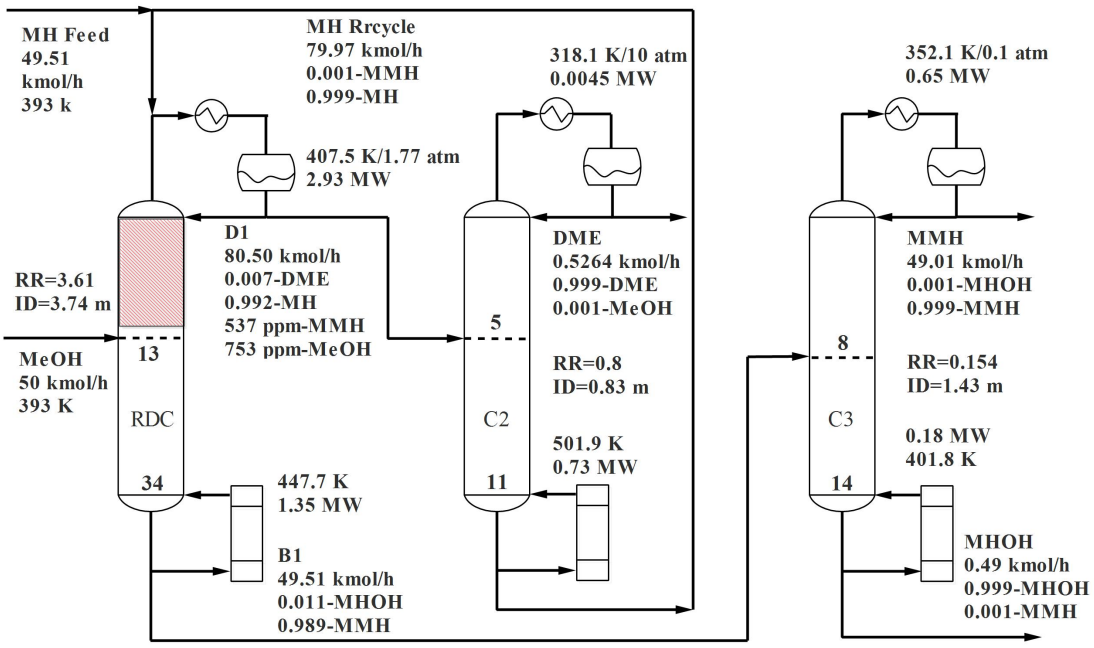

Fig. 1. Existing MMH process using the RD configuration

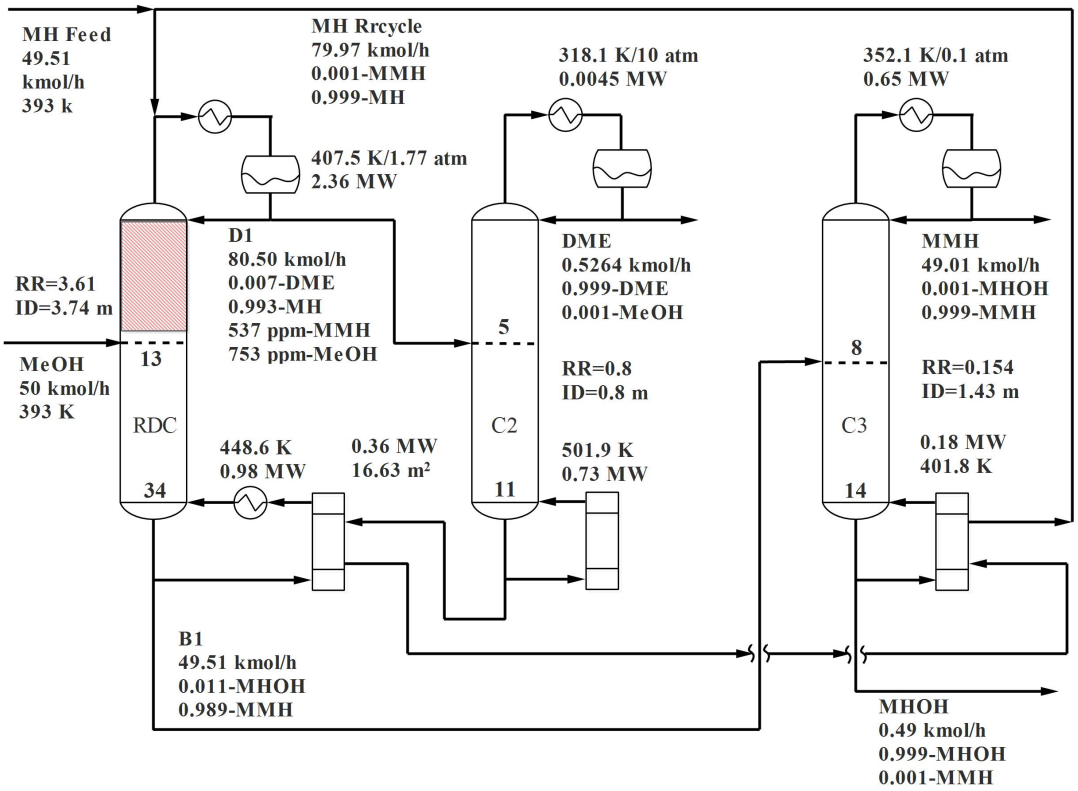

Fig. 2. Existing MMH process by the RD with heat integration

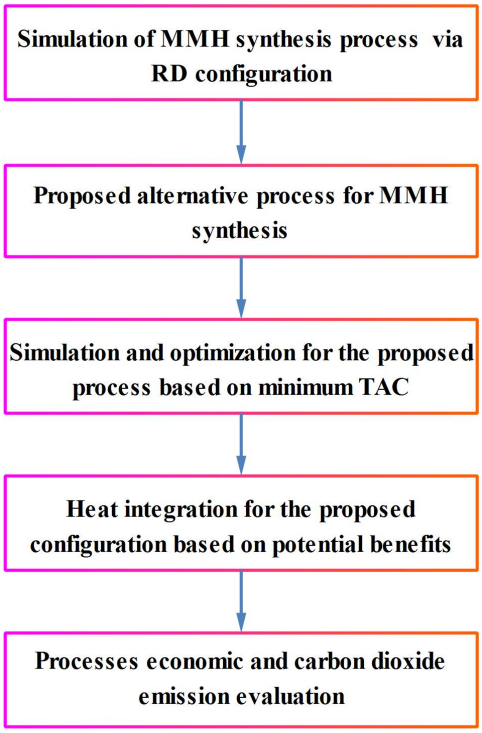

Fig. 3. Proposed procedure for optimal design of MMH production process using DPTCRD technology

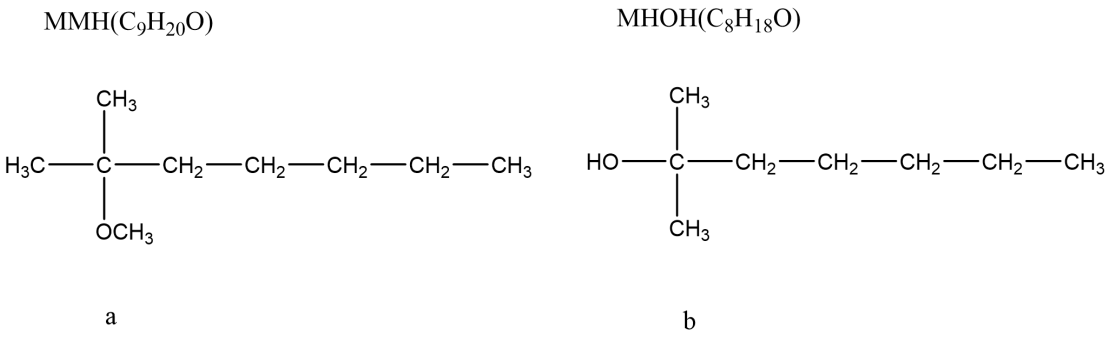

Fig. 4. Molecular structures of MMH and MHOH

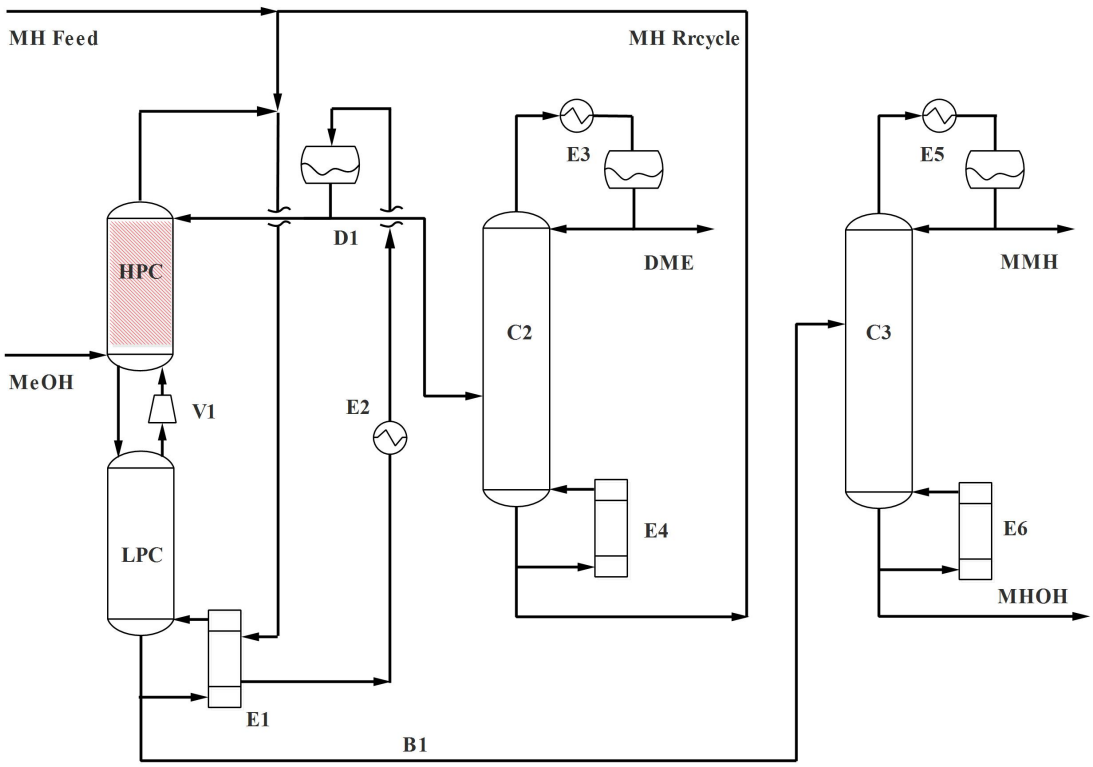

Fig. 5. The proposed DPTCRD process for the synthesis of MMH

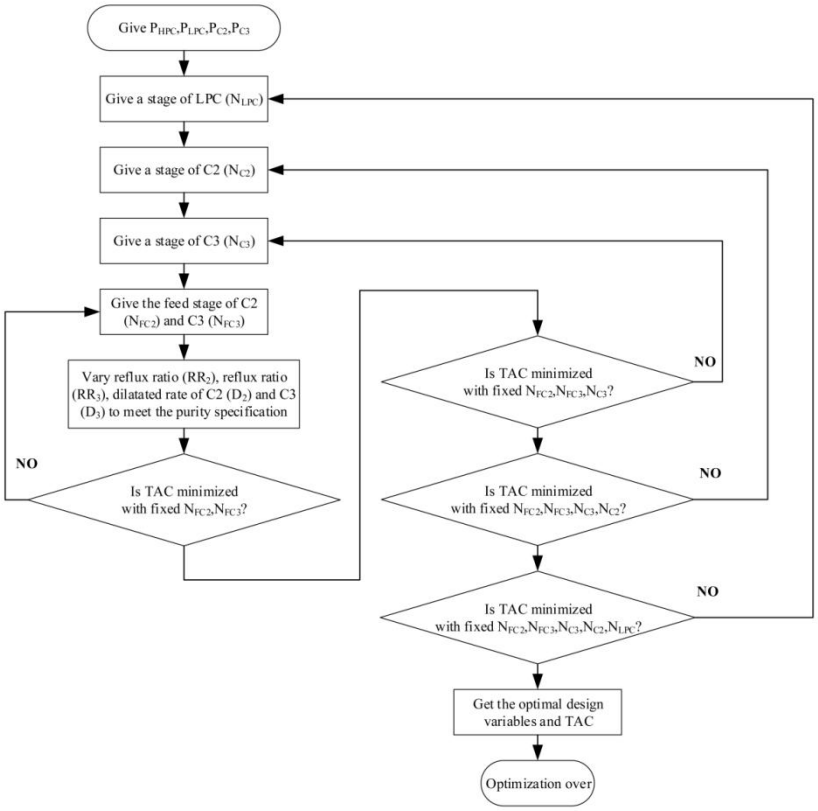

Fig. 6. Sequential iterative optimization procedure of DPTCRD process

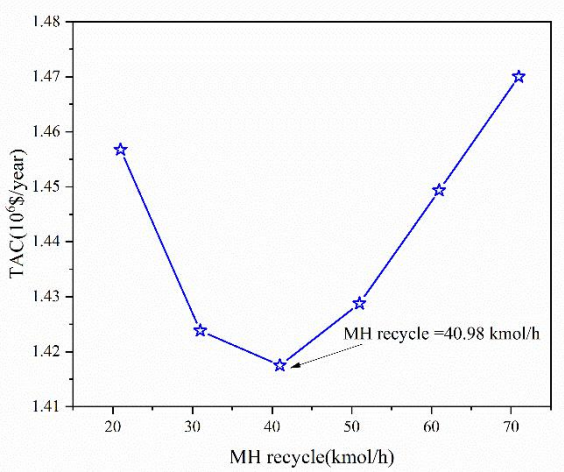

Fig. 7. The effect of MH recycle rate on the TAC

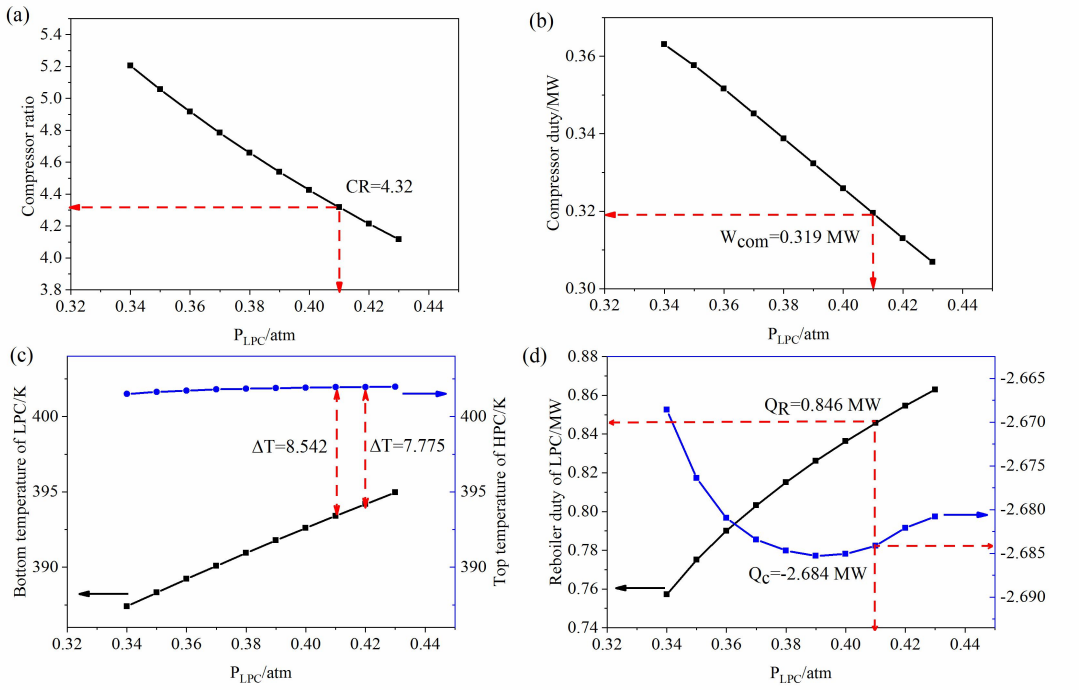

Fig. 8. Effects of operation pressure in LPC on (a) compress ratio (b) compressor duty (c) heat transfer temperature difference (d) condenser duty of the HPC and reboiler duty of the LPC

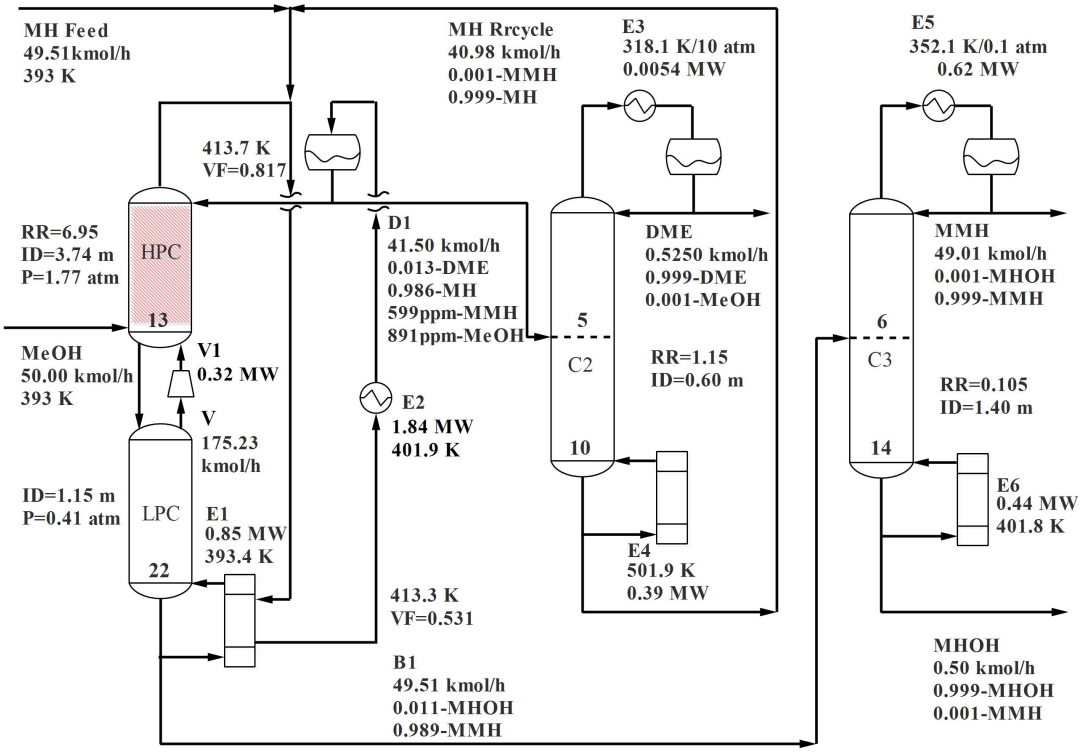

Fig. 9. The optimal DPTCRD configuration for the MMH production

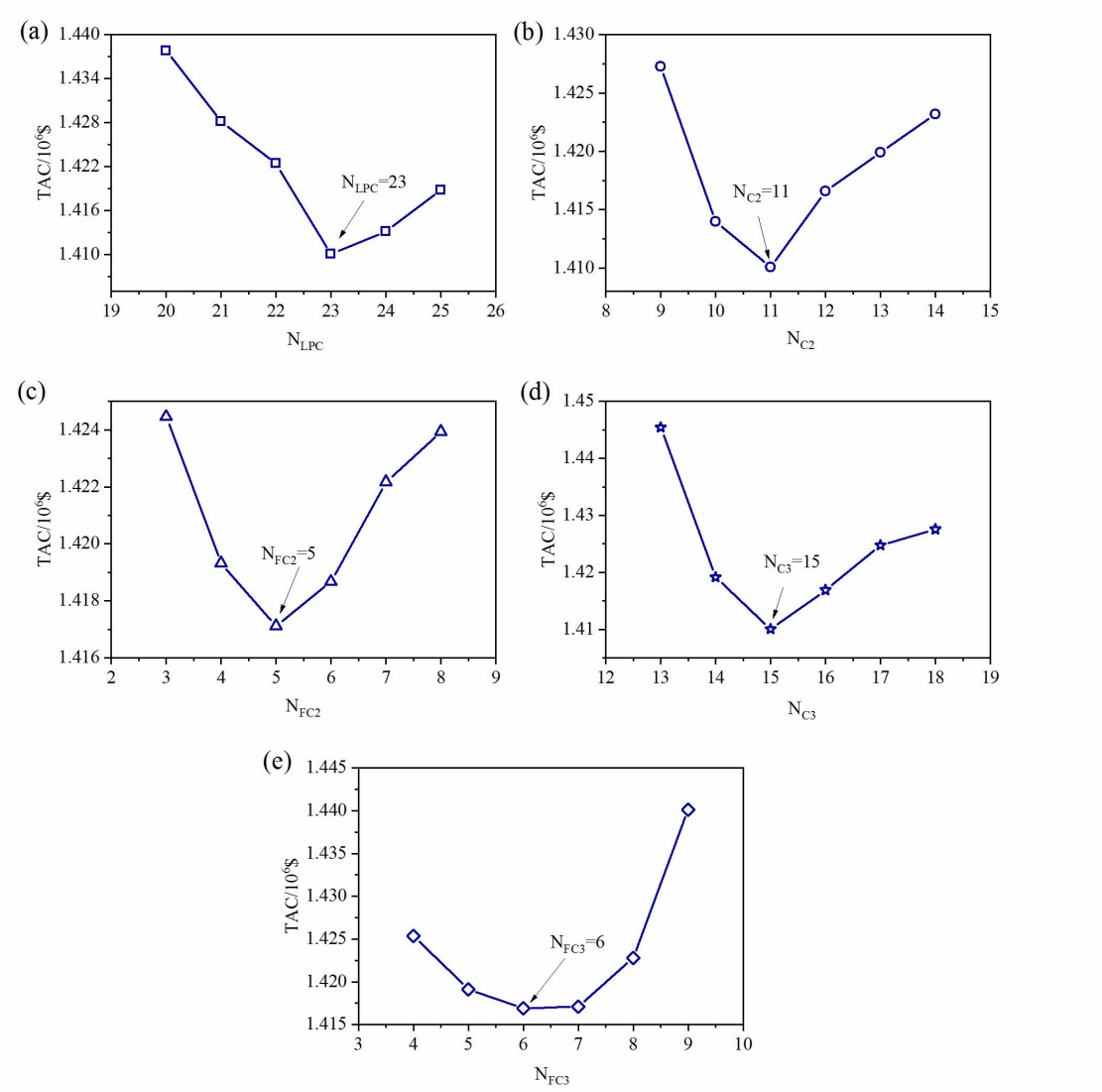

Fig. 10. The effects of (a) the total stages of LPC (N_{LPC}), (b) the total stages of C2 (N_{C2}), (c) the total stages of C3 (N_{C3}), (d) the feed locations of C2 (N_{FC2}) and (e) C3 (N_{FC3}) on the TAC

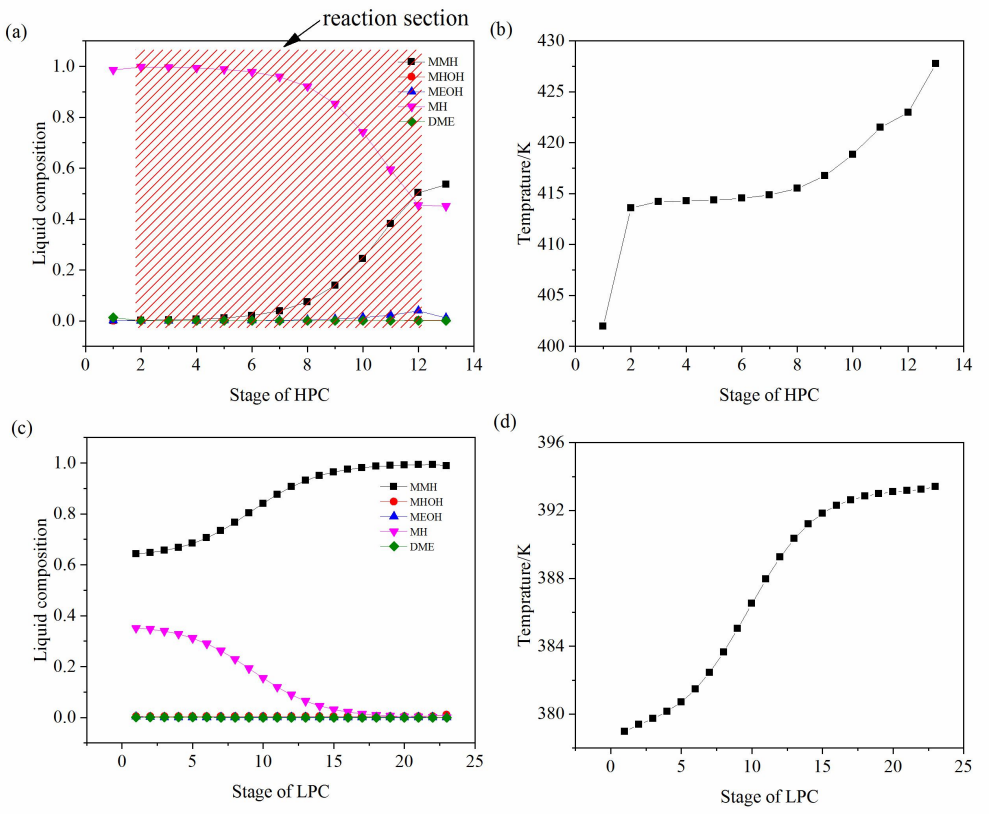

Fig. 11. Liquid composition and temperature profiles in (a, b) HPC and (c, d) LPC

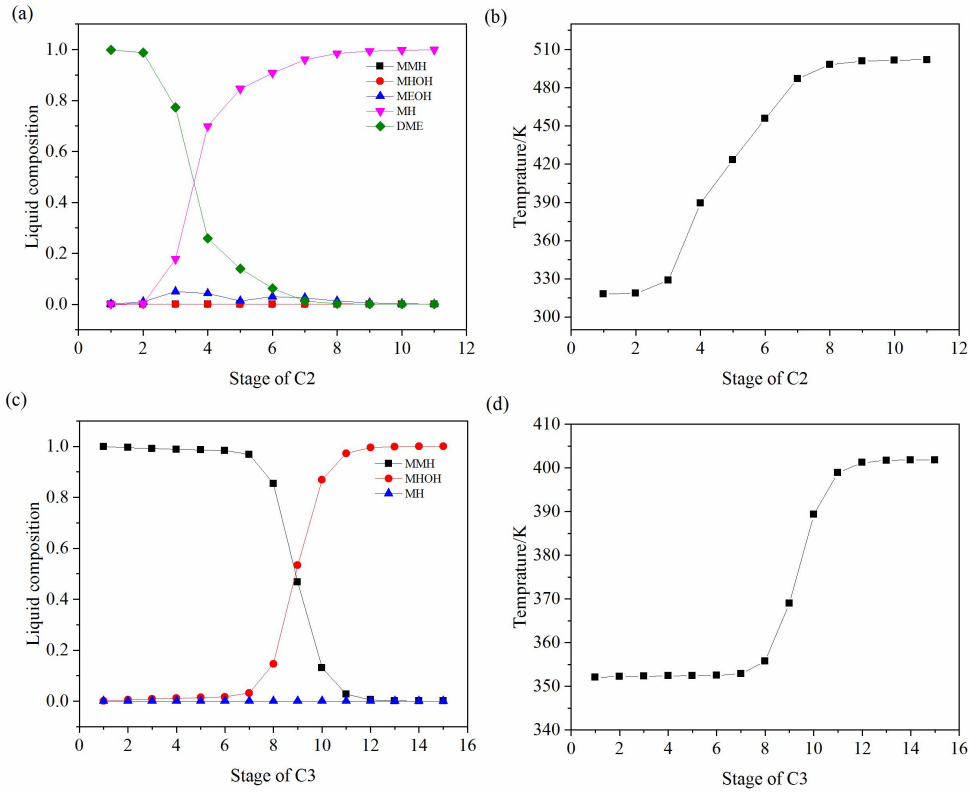

Fig. 12. Liquid composition and temperature profiles of (a, b) C2 and (c, d) C3

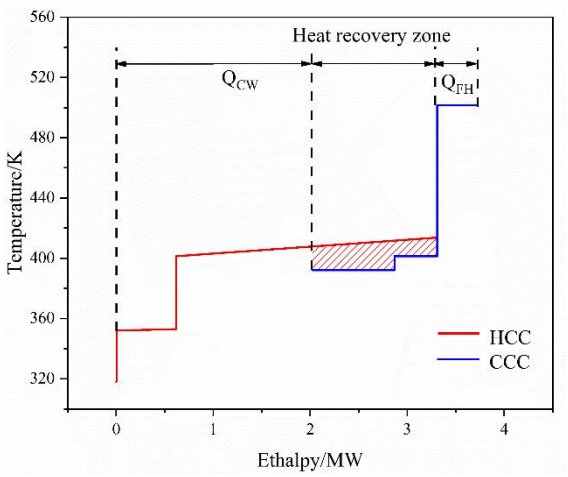

Fig. 13. Temperature-enthalpy diagram of the DPTCRD process

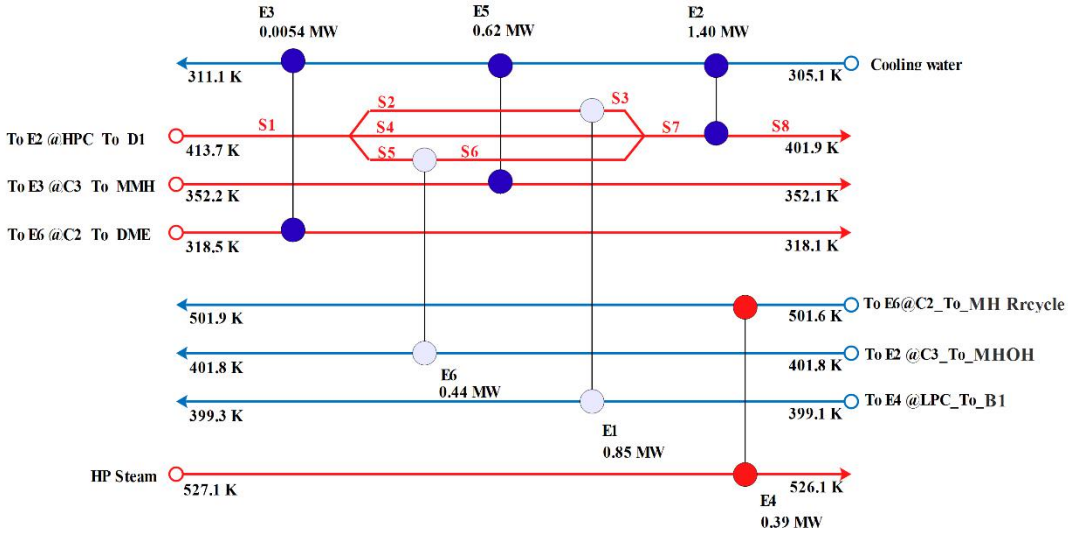

Fig. 14. The final heat exchanger network of the DPTCRD process

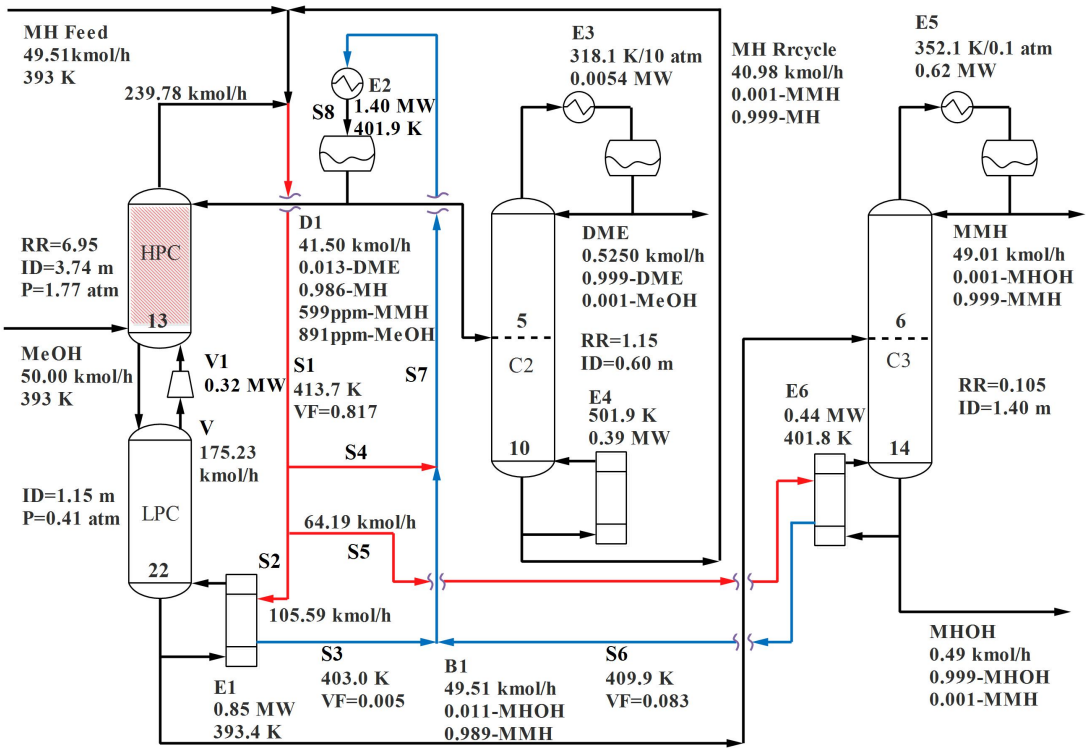

Fig. 15. The optimal flowsheet of HI-DPTCRD process

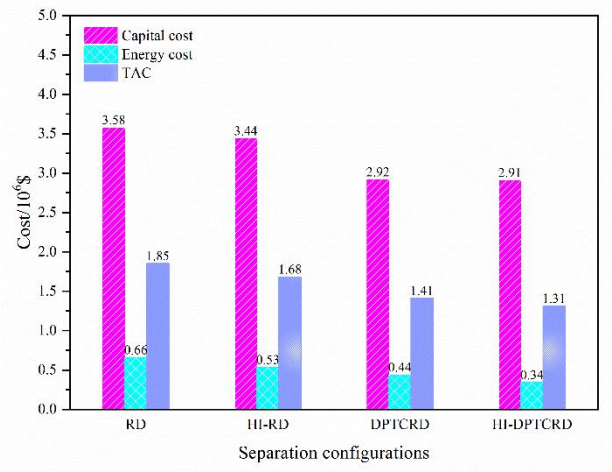

Fig. 16. Economic comparisons of the RD, DPTCRD and HI-DPTCRD processes

Table 1. Kinetic parameters from Griffin et.al [4]

parameters	unit	r_1		r_2
		forward	reverse	
k (overall reaction rate)	$kmol \cdot s^{-1} \cdot kg^{-1}cat$	6.7×10^{7}	2.1×10^{-6}	1.3×10^{9}
E	$kJ \cdot kmol^{-1}$	90000	900	105900
concentrations	mole fraction	$x_{MH}\,x_{MeOH}$	x_{MMH}	$(x_{MeOH})^2$

Table 2. Simulation parameters of RD process

parameter	reactive distillation column	C2	C3
number of stages	35	12	15
feed locations	13/1	5	8
reaction section	2-12	-	-
reflux ratio	3.61	0.80	0.16
pressure (atm)	1.77	10.00	0.10
liquid holdup (m^3)	0.75	-	-

Table 3. Basis of economics and equipment sizing

column diameter (*d*): Aspen Plus tray sizing
column height (*h*): N_T trays with 2 *ft* spacing plus 20% extra length
column and other vessel (*d* and *h* are in meters)

$$\text{capital cost }(\$) = \left(\frac{M\ \&\ S}{280}\right) \times 937.64 \times d_{col}^{1.006} \times h_{col}^{0.802} \times (2.18 + 3.67)$$

column Tray (*d* and *h* are in meters)

$$\text{capital cost }(\$) = \left(\frac{M\ \&\ S}{280}\right) \times 97.24 \times d^{1.55} \times h_{tray} \times (1.0 + 1.7)$$

reboilers (area in m^2)

heat-transfer coefficient = 0.568 kW/K·m^2
differential temperature = steam temperature − base temperature

$$\text{capital cost }(\$) = \left(\frac{M\ \&\ S}{280}\right) \times 474.67 \times A^{0.65} \times 7.35$$

coolers (area in m^2)

heat-transfer coefficient = 0.852 kW/K·m^2
differential temperature = [a]LMTD of (inlet or outlet temperature −315 K)

$$\text{capital cost }(\$) = \left(\frac{M\ \&\ S}{280}\right) \times 474.67 \times A^{0.65} \times 5.29$$

heat exchanger (area in m^2)

heat-transfer coefficient = 0.852 kW/K·m^2
differential temperature = [a]LMTD of inlet or outlet temperature

$$\text{capital cost }(\$) = \left(\frac{M\ \&\ S}{280}\right) \times 474.67 \times A^{0.65} \times 5.29$$

compressor

$$\text{capital cost }(\$) = \left(\frac{M\ \&\ S}{280}\right) \times 410.85 \times bp^{0.82} \times (2.18 + 1)$$

energy cost

low pressure steam = \$7.78/GJ (5 bar, 160 °C)
medium pressure steam = \$8.22/GJ (5 bar, 184 °C)
high pressure steam = \$9.88/GJ (5 bar, 254 °C)
electricity = \$16.80/GJ

cooling water = $ 0.354/GJ (32 to 40 °C)
catalyst cost=$10/kg

[a]LMTD: logarithmic mean temperature difference; [b]bp represents power of compressor.

Table 4. Economic comparison of four configurations for MMH production process

		RD	HI-RD	DPTCRD	HI-DPTCRD
RDC/HPC	shell cost (10^6 $)	2.003	2.003	0.816	0.816
	HX cost (10^6 $)	0.788	0.666	0.096	0.080
	EC(10^6 $)	0.343	0.259	0.019	0.019
LPC	shell cost (10^6 $)	-	-	0.327	0.327
	HX cost (10^6 $)	-	-	-	-
	EC(10^6 $)	-	-	-	-
C2	shell cost (10^6 $)	0.116	0.116	0.064	0.064
	HX cost (10^6 $)	0.237	0.237	0.165	0.165
	EC(10^6 $)	0.203	0.203	0.110	0.110
C3	shell cost (10^6 $)	0.266	0.266	0.242	0.242
	HX cost (10^6 $)	0.166	0.083	0.228	0.082
	EC(10^6 $)	0.046	0.006	0.103	0.006
heat exchanger	CC (10^6 $)	-	0.067	0.205	0.359
	EC(10^6 $)	-	-	-	-
compressor	CC (10^6 $)	-	-	0.774	0.774
	EC(10^6 $)	-	-	0.140	0.140
catalyst cost ($10^6$$)		0.066	0.066	0.066	0.066
total CC(10^6 $)		3.576	3.439	2.917	2.909
total EC (10^6 $/y)		0.659	0.534	0.438	0.341
TAC(10^6 $/y)		1.851	1.681	1.410	1.311
TAC saving (%)			9.18	23.80	29.17

Table 5. Comparison of the CO_2 emissions of the four processes

	devices	RD	HI-RD	DPTCRD	HI-DPTCRD
energy (MW)	reboiler 1	1.35	0.98	-	-
	reboiler 2	0.73	0.73	0.39	0.39
	reboiler 3	0.18	-	0.44	-
$(CO_2)_{emissions,S}$ (kg/h)		764.00	578.07	280.58	131.84
electrical (MW)	compressor	-	-	0.32	0.32
$(CO_2)_{emissions,E}$ (kg/h)		-	-	58.88	58.88
total $(CO_2)_{emissions}$ (kg/h)		764.00	578.07	339.46	190.72
saving (%)		0.00	24.34	55.57	75.04